Vacuolization and alterations of lysosomal membrane proteins in cochlear marginal cells contribute to hearing loss in neuraminidase 1– deficient mice

Xudong Wu, Katherine A. Steigelman, Erik Bonten, Huimin Hu, Wenxuan He, Tianying Ren, Jian Zuo, Alessandra d'Azzo

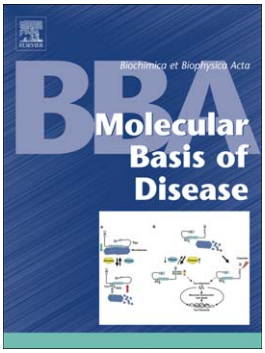

Vacuolization and alterations of lysosomal membrane proteins in cochlear marginal cells contribute to hearing loss in neuraminidase 1– deficient mice

Xudong Wu, Katherine A. Steigelman, Erik Bonten, Huimin Hu, Wenxuan He, Tianying Ren, Jian Zuo, Alessandra d'Azzo

PII: S0925-4439(09)00244-0
DOI: doi:10.1016/j.bbadis.2009.10.008
Reference: BBADIS 63024

To appear in: *BBA - Molecular Basis of Disease*

Received date: 13 July 2009
Revised date: 28 September 2009
Accepted date: 16 October 2009

Please cite this article as: Xudong Wu, Katherine A. Steigelman, Erik Bonten, Huimin Hu, Wenxuan He, Tianying Ren, Jian Zuo, Alessandra d'Azzo, Vacuolization and alterations of lysosomal membrane proteins in cochlear marginal cells contribute to hearing loss in neuraminidase 1– deficient mice, *BBA - Molecular Basis of Disease* (2009), doi:10.1016/j.bbadis.2009.10.008

BBA Molecular Basis of Disease

Vacuolization and alterations of lysosomal membrane proteins in cochlear marginal cells contribute to hearing loss in neuraminidase 1– deficient mice

Xudong Wu[1, 3], Katherine A Steigelman[1, 3], Erik Bonten[2], Huimin Hu[2], Wenxuan He[4], Tianying Ren[4], Jian Zuo[1*], Alessandra d'Azzo[2*]

[1]Department of Developmental Neurobiology and [2]Department of Genetics and Tumor Cell Biology, St Jude Children's Research Hospital, Memphis, TN, USA

[3]Department of Anatomy and Neurobiology and Integrated Program in Biomedical Sciences, University of Tennessee Health Science Center, Memphis, TN 38163, USA [4]Oregon Hearing Research Center, Oregon Health & Sciences University, Portland, OR 97239, USA

*Corresponding authors: Jian.zuo@stjude.org , 262 Danny Thomas Place ms 322, Memphis, TN, 38105, (901) 595-3891 and fax (901) 595-2270

sandra.dazzo@stjude.org, 262 Danny Thomas Place ms 331, Memphis, TN, 38105, (901) 595-2698 and fax (901) 595-6035

Abstract

The neuraminidase-1 (*Neu1*) knockout mouse model is a phenocopy of the lysosomal storage disease (LSD) sialidosis, characterized by multisystemic and neuropathic symptoms, including hearing loss. We have characterized the auditory defects in $Neu1^{-/-}$ mice and found that hearing loss involves both conductive and sensorineural components. Auditory brainstem response (ABR) thresholds were significantly elevated in $Neu1^{-/-}$ mice at P21 (48~55 dB), and hearing loss appeared progressive (ABR threshold elevation 53~66 dB at P60). At these ages $Neu1^{-/-}$ mice accumulated cerumen in the external ear canal and had a thickened mucosa and inflammation in the middle ear. In cochleae of adult wild-type mice, Neu1 was expressed in several cell types in the stria vascularis, the organ of Corti, and spiral ganglion. Progressive morphological abnormalities such as extensive vacuolization were detected in the $Neu1^{-/-}$ cochleae as early as P9. These early morphologic changes in $Neu1^{-/-}$ cochleae were associated with oversialylation of several lysosomal associated membrane proteins (Lamps) in the stria vascularis. A marked increase in the expression and apical localization of Lamp-1 in marginal cells of the stria vascularis predicts exacerbation of lysosomal exocytosis into the endolymph. Consequently, the endolymphatic potential in $Neu1^{-/-}$ mice was reduced by approximately 20 mV at ages P31–P44, which would cause dysfunction of transduction in sensory hair cells. This study suggests a molecular mechanism that contributes to hearing loss in sialidosis and identifies potential therapeutic targets.

INTRODUCTION

Neuraminidase-1 (NEU1) initiates the intralysosomal hydrolysis of sialo-oligosaccharides, glycolipids, and glycoproteins by removing their terminal sialic acid residues. In human and murine tissues, NEU1 forms a high molecular weight complex (>1000 kDa) with at least 2 other proteins – β-galactosidase (β-gal) and the protective protein cathepsin A (PPCA) [1]. In lysosomes, NEU1 and β-gal are dependent on PPCA for the acquisition of catalytic activity and to maintain a stable conformation. Whereas NEU1 activity is exclusively present in the high molecular weight complex, PPCA and β-gal activities are also present in a lower molecular weight complex (~700 kDa) and as free forms [2].

Deficiency of NEU1 is associated with 2 neurodegenerative autosomal recessive lysosomal storage diseases (LSDs): sialidosis, caused by structural lesions in the lysosomal NEU1 locus on chromosome 6p21 [3], and galactosialidosis (GS), a combined deficiency of NEU1 and β-gal caused by mutations in the *PPCA* gene on chromosome 20q13.1 [1]. Patients with sialidosis are characterized by multiple phenotypes, which are classified according to the age of onset and severity of symptoms, and usually correlate with the level of residual enzyme activity [4]. Type I sialidosis (or cherry-red spot/myoclonus syndrome) is an attenuated form of the disease that has an onset in the second decade of life and is associated with progressive vision loss, hearing loss, nystagmus, ataxia, and grand mal seizures [3]. Type II sialidosis, a severe form of the disease, is subdivided into 3 groups: congenital or hydropic (in utero), infantile (onset within first year of life), and juvenile (onset in first or second decade of life) [3]. The congenital form is associated with either hydrops fetalis and stillbirth or neonatal ascites and death at an early age [3]. Type II sialidosis may also be associated with symptoms such as facial edema, inguinal hernias, hepatosplenomegaly, and stippling of the epiphyses. Patients with Type II sialidosis patients who survive longer develop a progressive mucopolysaccharidosis-like

phenotype, which includes coarse facies, visceromegaly, dysostosis multiplex, vertebral deformities, mental retardation, and cherry-red spot/myoclonus [3, 5-7].

Auditory deficits are common in patients with LSDs [8-10] . β-glucuronidase–deficient mice, which serve as a model for the LSD mucopolysaccharidosis VII (MPSVII) or Sly disease, have been shown to have sensorineural defects in the inner ear as well as conductive abnormalities in the middle and external ears, which contribute to hearing loss [11, 12]. Interestingly, although pronounced lysosomal storage has been observed in many cell types in the inner ear of MPSVII mice, no obvious loss of hair cells or ganglion cells has been detected [11, 12]. The molecular mechanism of sensorineural hearing defects in this mouse model and in LSD patients in general remains unclear.

Cochlear duct consists of three fluid-filled compartments: the scala vestibuli, the scala media, and the scala tympani. The scala vestibuli and the scala tympani are filled with perilymph, a fluid whose ionic composition is similar to that of cerebrospinal fluid (reviewed in [13]). Endolymph is the fluid within the scala media, which is sealed by virtue of tight junctions between adjacent cells including the sensory hair cells that line its boundaries (reviewed in [13]). Many sensorineural defects in the inner ear are related to the dysfunction of homeostasis of the endolymph [14, 15]. Endolymph contains high concentration of potassium, which is pumped mainly by the stria vascularis, a highly vascularized epithelium lining along the lateral part of scala media (reviewed in [13]). The stria vascularis is composed of three layers of cells: marginal cells, intermediate cells, and basal cells (reviewed in [13]). The transportation of potassium into the scala media by the stria vascularis is against the ionic gradient and thus builds up a high potassium concentration (approximate 160 mM) and positive endolymphatic potential (EP, approximate 90 mV) surrounding the scala media [16]. The pH value of endolymph is

maintained at 7.4 under physiological conditions [16]. Injection of acetazolamide to scala media to acidify the endolymph caused reduction of EP [17].

Neu1-knockout mice lack Neu1 activity and have been shown to develop a severe sialidosis phenotype [18, 19]. These mice exhibit age-dependent extramedullary hematopoiesis caused by increased lysosomal exocytosis in the bone niche, resulting from oversialylation of the lysosomal-associated membrane protein-1 (Lamp-1), a primary player in this process [19]. In this study, we have characterized the auditory defects in *Neu1*$^{-/-}$ mice, which display a profound hearing loss as early as P21. We found that hearing loss in *Neu1*$^{-/-}$ mice involves both conductive and sensorineural components. The loss of *Neu1* activity and its effect on Lamp-1, which in turn exacerbates lysosomal exocytosis, provides a mechanism for how progressive hearing loss occurs in *Neu1*$^{-/-}$ mice. Our studies in the *Neu1* knockout mouse model put forward a molecular mechanism that may contribute to hearing loss in NEU1 deficient patients and identify potential therapeutic targets for treatment of this severe condition.

RESULTS

Hearing loss in *Neu1*$^{-/-}$ mice

We examined the auditory function of *Neu1*$^{-/-}$ mice by analyzing ABR thresholds at different ages. At P21, a significant elevation in ABR thresholds was recorded in null mice compared to wild-types, which ranged from 48 to 55 dB for click, 8, 16, and 32 kHz tone stimuli, respectively (**Fig. 1 A, B)**. Hearing loss appeared to be progressive as ABR thresholds at all stimuli were significantly higher in *Neu1*$^{-/-}$ mice at age P60 (for click stimuli: $P<0.05$, Student's t-test; for

tone stimuli; P<0.001, two way ANOVA) **(Fig. 1 A, B)**. However, there were no significant threshold elevations in *Neu1*$^{+/-}$ mice at all ages tested (data not shown).

Morphologic changes in the external and middle ears of *Neu1*$^{-/-}$ mice

To determine whether abnormalities in the middle and external ears could cause hearing loss in *Neu1*$^{-/-}$ mice, we performed a histologic analysis of H&E stained tissue sections from mice at age P21 and P60. In contrast to wild-type mice, *Neu1*$^{-/-}$ mice accumulated cerumen in the external ear canal at P21 (**Fig. 2A** and **C**, and data not shown). *Neu1*$^{-/-}$ mice had a thickened mucosa lining the middle ear surface of the tympanic bulla **(Fig. 2C)**. Cells resembling those present in a typical chronic inflammatory responses [12, 20] had invaded but not filled the tympanic cavity **(Fig. 2D)**. The middle ear ossicles were over-ossified and showed a darker H&E staining pattern than that of wild-type littermates **(Fig. 2C)**. At P60, abnormalities in the external and middle ear had substantially progressed in *Neu1*$^{-/-}$ mice. The mice displayed a thickened cerumen occlusion in the external auditory canal in addition to severe otitis media **(Fig. 2G)**. The middle ear ossicles were completely encased in connective tissue, which had been infiltrated with different types of chronic inflammatory-appearing cells **(Fig. 2H)**. In addition, sclerosis marked by irregular-shaped lacunae surrounded by dark-blue bony ring was occasionally observed in the ossicles by H&E staining **(Fig. 2G, H)**. These morphological abnormalities found in the ear of *Neu1*$^{-/-}$ mice are consistent with previous reports of other LSD models [11, 12, 20].

Morphologic changes in cochleae of *Neu1*$^{-/-}$ mice

To investigate the potential involvement of inner ear sensory epithelia in the hearing loss seen in *Neu1*$^{-/-}$ mice, we examined the expression pattern of Neu1 in P21 cochleae by

immunohistochemistry (**Fig. 3**). Neu1 was most abundant in interdental cells, external sulcus cells, and ganglion cells. Staining was low in marginal cells, inner and outer pillar cells, Boettcher cells and faint in inner and outer hair cells and some fibrocytes in the spiral ligament.

At P9, P21, and P60, there were morphologic abnormalities in multiple cell types in *Neu1*$^{-/-}$ cochleae. At P9, toluidine blue staining of semi-thin plastic sections showed no obvious abnormality in the *Neu1*$^{-/-}$ cochlea, except for slight vacuolization in marginal cells of the stria vascularis (data not shown). However, by P21, vacuolization was apparent in many cell types (**Fig. 4B, C, D, E, F**), with the most extensive vacuolization in marginal cells and external sulcus cells. Moderate vacuolization was observed in both endothelial and mesothelial cells of Reissner's membrane, inner sulcus cells, Boettcher cells, outer hair cells, type-IV fibrocytes of spiral ligament, spiral prominence, interdental cells, and mesothelial cells lining in the perilymphatic side of the basilar membrane. Although wild-type ganglion cells expressed high levels of Neu1 **(Fig. 3E)**, vacuolization was detectable in *Neu1*$^{-/-}$ mice only at P60 but not P21 (**Fig. 4E**, and data not shown). Glial cells did not show recognizable vacuolization. Interestingly, there was no loss of hair cells or ganglion cells in *Neu1*$^{-/-}$ mice at both P21 and P60.

Since the most prominent morphologic changes occurred in marginal cells of the stria vascularis in *Neu1*$^{-/-}$ cochleae, morphologic changes in these cells were further examined at the ultrastructural level (**Fig. 5**). As early as P9, numerous vesicles approached to or docked at the apical surface of the marginal cells facing the scala media. At P21, vacuolization of marginal cells caused distention of these cells as well as a several fold increase in their size compared with wild-type cells. At P21, appearance of stereocilia in cochleae of *Neu1*$^{-/-}$ mice and wild-type littermates were similar under SEM (data not shown), indicating that the morphologic integrity of the mechanoelectrotransducer remained unchanged. The apical surface of marginal cells in the

stria vascularis of wild-type mice was smooth and filled with microvilli (**Fig. 6A**), whereas that of *Neu1*$^{-/-}$ mice showed many invaginations and cavities, indicative of excessive exocytosis/endocytosis of vesicles into the endolymph (**Fig. 6B, C**).

Lysosomal membrane proteins in cochleae of *Neu1-/-* mice

The earliest morphologic changes detected in the cochlea of *Neu1*$^{-/-}$ mice were the numerous vesicles approaching to and docking at the apical surface of marginal cells in the stria vascularis at P9–P21. We have previously shown that Lamp-1 is a natural substrate for Neu1 and is involved in lysosomal exocytosis. Hypersialylation of Lamp-1 in *Neu1*$^{-/-}$ macrophages and patients' fibroblasts has been shown to cause an increase in the number of docked lysosomes at the plasma membrane [19]. We therefore studied whether similar posttranslational modifications also occurred in cells of the *Neu1*$^{-/-}$ cochleae. Western blot analysis of cochlear lysates at P21 showed that there was a marked increase in the protein levels of Lamp-1 (2.98 fold) and Lamp-2 (3.19 fold) (**Fig. 7,** left panel). In contrast, no obvious increase (1.02 fold) was observed in the expression of Lamp-3, but its molecular weight was slightly higher than in cochleae of wild-type mice (**Fig. 7,** left panel). The lysosomal membrane protein Limp II was slightly more abundant (1.46 fold) in the knock-out lysate, while the lowest molecular weight band detected in the wild-type was absent in the *Neu1*$^{-/-}$ sample (**Fig. 7**, left panel). There was no overt difference in molecular weights and expression levels of several lysosomal and plasma membrane (PM) proton-pump and ion channel proteins (Na^+-K^+ ATPase B1 subunit, KCNQ1, TRPV5/6), but the V-ATPase subunit B1 was more abundant in cochlear lysates from *Neu1*$^{-/-}$ mice (2.35 fold) (**Fig. 7,** left panel; data not shown). V-ATPase is a major lysosomal membrane protein that pump protons into the lysosomes and maintains the acidic environment of lysosomes [21].

Immunohistochemical analysis of the stria vascularis from cochlear sections of P21 mice (**Fig. 7,** right panel) corroborated the protein expression. Expression levels of both Lamp-1 and -2 increased markedly at the apical membrane of marginal cells in the cochlea of *Neu1*$^{-/-}$ mice compared with wild-type cells, consistent with an increase in the number of lysosomes approaching to and docking at the PM. LIMP II expression level was slightly higher in *Neu1*$^{-/-}$ mice. As a control, we checked other membrane proteins (KCNQ1, Na^+-K^+ ATPase B1 subunit) in which no change would be expected. These membrane proteins indeed showed no substantial differences in expression levels or localization in the stria vascularis of *Neu1*$^{-/-}$ and wild-type mice (**Fig. 7,** right panel; data not shown).

Measurement of EP

The presence of numerous vesicles at the apical membrane of the marginal cells was a feature unique of the *Neu1*$^{-/-}$ cochlea. The increase in hypersialylated Lamp-1 and -2 in these cells at the same location suggested that these vesicles were PM-docked lysosomes [19]. Recently, we have shown that an increase in the sialylation and quantity of Lamp-1 in several *Neu1*$^{-/-}$ cell types correlated with enhanced lysosomal exocytosis [19]. Based on the accumulated evidence, we postulated that such phenotype could also occur in the *Neu1*$^{-/-}$ cochlea. Our prediction was that the excessive discharge of acidic lysosomal content into the endolymph would decrease both the pH and the EP of the endolymph. Unfortunately, direct measurement of pH in the endolymph is technically very difficult and prone to artifacts, because the total volume of endolymph is only approximately 0.19 µl per cochlea in the mouse [22]. However, we directly measured the EP in the basal turn of *Neu1*$^{-/-}$ mice and control littermates and found that the EP was significantly lower (~20 mV) in *Neu1*$^{-/-}$ mice at ages P31 and P44 compared to wild-type littermates (**Fig. 8**). This decrease would, in turn, cause a reduction in the electrical gradient across the

mechanoelectrotransduction channels of hair cells and could contribute to the progressive hearing loss seen in *Neu1*$^{-/-}$ mice.

DISCUSSION

The loss of Neu1 activity and its effect on Lamp-1 provides a mechanism for the occurrence of the profound and progressive hearing loss in *Neu1*$^{-/-}$ mice. Whether the same or a similar pathologic mechanism(s) is responsible for hearing loss in mouse models of seemingly unrelated LSDs and in patients with LSDs remains to be studied. The sensory apparatus of the inner ear is well suited for unraveling the pathologic mechanisms of hearing loss in LSDs because of the sensitivity of in vivo hearing measurements currently available, the enclosed nature of the cochlear compartment, and the knowledge of molecular pathways involved in auditory signal transduction. To date, hearing loss has been studied in only some mouse models of LSD, but these have given little information about potential molecular mechanisms [9, 11, 12, 20, 23-25]. Characterization of abnormalities present in the external, middle, and inner ears of *Neu1*$^{-/-}$ mice in our study provides for the first time a molecular mechanism by which the deficiency of a lysosomal hydrolase may cause hearing loss.

Consistent with studies of other mouse models of LSDs [9, 11, 12, 20, 23-25]; we have demonstrated that hearing loss in *Neu1*$^{-/-}$ mice involves both conductive and sensorineural components. In P60 mice, severe abnormalities in both the external and middle ears indicated the existence of conductive hearing loss. In younger mice (P21), these abnormalities were relatively mild; however, a significant 48~55 dB elevation of ABR thresholds were already evident at this early age. This inconsistency between the abnormalities in the external and middle ears and the

amount of hearing loss indicates that hearing impairment in *Neu1*$^{-/-}$ mice is preceded by structural defects of sensorineural components.

Various cell types in the inner ear exhibited vacuolization in *Neu1*$^{-/-}$ mice at P21. Similar to other LSD mouse models, vacuolization was mainly found in cell types that are responsible for the ionic homeostasis of endolymph such as inner sulcus cell, external sulcus cells, fibrocytes of spiral ligament, cells of Reissner's membrane, and inter-dental cells [11, 12, 23-25]. However, the early onset of drastic vacuolization in marginal cells of the stria vascularis in *Neu1*$^{-/-}$ mice was a unique feature [11, 12, 20, 23-25].

Interestingly, we did not find any notable hair cell degeneration at ages as old as P60 in *Neu1*$^{-/-}$ mice, although vacuolization was visible in outer hair cells (OHCs). OHC degeneration has not been detected in most LSD models except in the MPS I mice at 1 year of age [11, 12, 23-25]. In the mouse models of Pompe's disease, OHC vacuolization had no apparent effect on the hearing sensitivity [9]. Morphological change in OHC could also contribute to the hearing deficit in *Neu1*$^{-/-}$ mice.

Recent studies showed that only glial cells but not ganglion cells accumulated vacuolization in inner ears of MPS VII and MPS III mouse models whereas ASA$^{-/-}$ mice exhibited dramatic degeneration of cochlear ganglia [11, 24]. We also found vacuolization in ganglia in *Neu1*$^{-/-}$ mice at P60. Although the expression level of Neu1 in the ganglia is high in wild-type mice, spiral ganglion cells showed no overt vacuolization in *Neu1*$^{-/-}$ mice at P21. Therefore, dysfunction of ganglion cells might not be a major factor in the profound hearing loss observed in *Neu1*$^{-/-}$ mice at P21.

Additionally, vacuolization in mesothelial cells lining the basilar membrane could change the passive mechanical properties of cochlear partition and thus affect hearing sensitivity, as proposed from other LSD models [11, 24, 25].

Immunohistochemical analysis showed that Neu1 is expressed in many cochlear cell types, which line the epithelial surface of the cochlear endolymphatic compartment. These cells are important to maintain homeostasis of water-ionic recycling of the cochlear fluid and production and maintenance of EP [13]. Therefore, the lack of Neu1 may influence endolymphatic compositions that ultimately may lead to the dysfunction of mechanoelectrotransduction in sensory hair cells. In the *Neu1*$^{-/-}$ cochlea at as early as P9 cytoplasmic vacuolization was already visualized mainly in marginal cells of the stria vascularis, which play crucial roles in maintaining endolymphatic compositions such as K^+ concentration and EP [13]. Therefore, the morphologic changes we detected in marginal cells of the inner ear of *Neu1*$^{-/-}$ mice are probably the earliest, and they further trigger subsequent alterations in inner ear endolymph.

We have recently shown that the deficiency of Neu1 causes the hypersialylation of Lamp-1 in bone marrow cells from *Neu1*$^{-/-}$ mice and fibroblasts from patients with sialidosis. This prolongs the half-life of Lamp-1 and results in an increase in docked lysosomes at the PM. The latter phenomenon is associated with abnormally high levels of lysosomes that exocytose their luminal content into the extracellular environment [19]. The numerous indentations and cavities present on the surface of the marginal cells facing the scala media in P21 *Neu1*$^{-/-}$ mice support the notion that active endocytosis or exocytosis, or both, are exacerbated in defective marginal cells at this early age. Furthermore, the marked increase of Lamp1- and -2 but not of plasma membrane proteins (Na-K ATPase B1 subunit, TRPV5, TRPV6 or KCNQ1) near the apical surface of marginal cells in cochleae of *Neu1*$^{-/-}$ mice could be indicative of increased exocytosis

of the luminal content into the endolymph. The release of large amount of hypersialylated lysosomal luminal content carrying negative charge would subsequently decrease the voltage potential inside the endolymph. Our hypothesis that this should result in a decrease in EP in *Neu1*$^{-/-}$ endolymph was indeed confirmed. However, this relatively moderate change in EP may not be sufficient to explain the substantial elevation (48~55 dB) of hearing threshold in the mutant mice, given the average empirical rate of 1 dB/mV [26].

The extensive apical vacuolization in marginal cells of *Neu1*$^{-/-}$ mice indicates that the hearing defect may be caused by acidic lysosomal components released from interdental and marginal cells. This would decrease the pH of the endolymph and eventually lead to impaired transduction of hair cells. Recent studies have shown that acidification of the endolymph can provoke an increase in the calcium concentration of the cochlear endolymph, causing a dysfunction in the mechanoelectrotransduction channel of hair bundles [27], and such defects could ultimately result in deafness in *Neu1*$^{-/-}$ mice.

The V-type ATPase B1 subunit is a major lysosomal membrane protein that pumps protons into the lysosomes and maintains the acidic environment [21]. In cochlea, V-ATPase is expressed in both interdental cells and cells of stria vascularis [28]. The increase in the expression of the V-ATPase B1 subunit in the cochleae of *Neu1*$^{-/-}$ mice may increase the transport of protons into the lysosomes, thereby increasing acidity. Mutations of the V-ATPase B1 subunit are known to cause sensorineural hearing loss in humans [26, 27], and several V-ATPase B1 mutant mice also display a hearing phenotype similar to *Neu1*$^{-/-}$ mice [28-30]. In contrast, V-ATPase B1 knockout mice do not exhibit any hearing phenotypes [29]. It is likely that the increase of V-ATPase B1 in *Neu1*$^{-/-}$ mice may represent an effective gain of function of V-ATPase B1. The increased expression of V-type ATPase B1 in the cochleae of *Neu1*$^{-/-}$ mice is

likely a compensatory effect to help maintain the intralysosomal acidity by increasing the influx of protons into lysosomes. Presumably, the large amount of negatively charged hypersialylated Lamp-1, Lamp2, and other unidentified targets of Neu1 would neutralize and potentially exceed the increased positive charge of protons by V-ATPase and convergently reduce the EP in *Neu1*$^{-/-}$ cochlea. Nevertheless, we cannot rule out a potential direct correlation between increased expression of V-ATPase B1 and hearing loss in *Neu1*$^{-/-}$ mice. This hypothesis can be tested by studying whether double-deficient V-ATPase B1/Neu1 mice have less severe hearing phenotypes than *Neu1*$^{-/-}$ mice do.

In conclusion, we have provided evidence that the lack of Neu1 and the potential exacerbation of lysosomal exocytosis in the inner ear play a role in the occurrence of hearing loss in *Neu1*$^{-/-}$ mice. **Figure 9** shows one of the crucial downstream cascades of events that contribute to the hearing phenotype. At P21, both conductive and neurosensory defects contribute to hearing loss in *Neu1*$^{-/-}$ mice. However, morphological changes such as the accumulation of cerumen in the external ear canal, thickened mucosa and inflammation in the middle ear are possibly sufficient to affect the efficiency of sound transfer. Second, vacuolization in outer hair cells could also impair the cochlear amplification. Third, in addition to marginal cells, vacuolization in other cells types that maintain ionic homeostasis of endolymph could also affect the hearing. Finally, all lysosomal storage in cochlear cells could also affect the passive mechanics of the basilar membrane and thus lead to a hearing deficit. At present, we cannot exclude the possibility that other mechanisms are also contributing to the loss of hearing in *Neu1*$^{-/-}$ mice, nor do we know whether the same factors underlie similar phenotypic alteration in other LSD animal models and patients. Nonetheless, the current findings set the basis for understanding the cause of hearing loss in NEU1 deficiencies and for developing therapeutic

interventions that may prevent or reverse this disease phenotype.

MATERIALS AND METHODS

Mouse genotyping

Neu1$^{-/-}$ mice were generated by targeted disruption of the *Neu1* locus, as previous reported [18], and maintained in an FVB genetic background. A PCR-based strategy was used to identify genotypes of Neu1-knockout mice from genomic DNA. Age-matched *Neu1*$^{-/-}$ and *Neu1*$^{+/+}$ controls from either littermate or different litters were used. All animal procedures were carried out in accordance with the US Public Health Service Policy on the Humane Care and Use of Laboratory Animals and were approved by the institutional animal care and use committees of the St. Jude Children's Research Hospital and the Oregon Health Sciences University.

ABR recording

The ABR assay was performed as described previously [31]. All data was analyzed by two way ANOVA or Student's t-test.

Electronic microscopy and preparation of samples

Tissues were briefly washed in 0.1 M PBS, post-fixed in 0.8% osmium tetroxide/3% ferrocyanide in 0.1 M PBS for 2 h, and washed with deionized distilled water. Tissues were then dehydrated by using a series of ascending concentrations of ethanol and stained en bloc with 2% uranyl acetate/100% ethanol under vacuum for 1 h at 60°C, embedded in Spurr's resin (Ted Pella, Redding, CA), and polymerized for 2 days at 60°C. Semi-thin sections (40 μm) were stained with 0.1% toluidine blue and photographed under a light microscope. Ultra-thin sections

(50 nm) were cut with a diamond knife, counterstained, and observed by transmission electron microscopy. For scanning electron microscopy (SEM), whole mounts of cochlear half-turns were critical-point dried, sputter-coated with platinum, and imaged with a Philips ESEM XL30 (FEI company, Netherlands).

Preparation of paraffin sections and hematoxylin and eosin (H&E) staining

Mice were intracardiacally perfused and fixed with 4% paraformaldehyde. The inner ears were isolated, postfixed, and decalcified in 120 mM EDTA (pH 7.2). For immunostaining of paraffin sections, the decalcified inner ear was transferred to 70% ethanol, dehydrated through a series of increasing gradients of ethanol, paraffinized, and embedded. A Richard-Allan microtome (Richard-Allan Scientific, Kalamazoo, MI) was used to cut 12 μm–thick sections of the inner ear. Paraffin sections were dehydrated by using xylene, a series of decreasing gradients of ethanol, hematoxylin, ammuno water, eosin, acidic alcohol, and an increasing gradient of ethanol, and then dried in xylene. Finally, slides were mounted and observed by light microscopy.

Immunohistochemical analysis

Immunostaining was performed on de-paraffinized sections. Briefly, slides were rinsed twice with 0.01 mM PBS, treated with 10 mM sodium citrate buffer (pH 6.0) at 85ºC for 15 min, blocked with blocking solution for 30 min at room temperature, and incubated with the primary antibody overnight at 4ºC. Slides were then rinsed 5 times with PBS. Biotin-labeled secondary antibodies (Vector Lab., Inc. Burlingame, CA) were added on the slides and incubated at room temperature for 1 h. The avidin–biotin complex solution was subsequently added and slides were

rinsed. DAB (KPL, Gaithersburg, MD) reactions were performed according to manufacturer's manual and monitored by light microscopy until desired staining was obtained.

Western blot analysis

Fresh cochleae isolated from mice were homogenized in lysis buffer [50 mM Tris-HCl (pH 7.5); 150 mM NaCl, 5mM EDTA (pH 8.0); 1% NP40; 5% glycerol, 1 mM DTT, 1 mM PMSF, 1× Complete cocktail (Rosch, Germany); 0.5 mM sodium vanadate, 10 mM NaF]. Lysates were loaded together with 4× Nupage LDS loading buffer (Invitrogen, Carlsbad, CA) and DTT (final concentration 100 mM) to the samples and incubated at 65ºC for 10 min and resolved on a 4–20% SDS-PAGE gel. The protein was then transferred to a polyvinylidene fluoride (PVDF) membrane and probed with Neu1 antibody [32], LAMP1 (clone 1D4B, BD Biosciences, San Diego, CA), LAMP2 (M3/84, Santa Cruz Biotechnology, Santa Cruz, CA), LAMP3 (H-193, Santa Cruz), LIMPII (N-18, Santa Cruz,), v-ATPase B1 (N-19, Santa Cruz), Na-K ATPase B1 (N-20, Santa Cruz), TRPV5 (CAT21-A, Alpha Diagnostic International, San Antonio, Texas), TRPV6 (CAT11-A, Alpha Diagnostic International), and KCNQ1 (H-130 and C-20, Santa Cruz) antibodies. For each antibody, 2 to 4 independent experiments from two sets of mice were used in western blot analysis. To ensure quantification of protein expression levels were within the linear range, we only chose a moderate exposed film from 4-5 different exposure time-points. The intensities of each band was measured using an Alpha DigDoc 1000 (Alpha Innotech Corporation, CA), subtracted background, and normalized to GAPDH.

Measurement of EP

The animal was anesthetized intramuscularly with 120 mg/kg ketamine and the animal's head was secured in a custom-made head holder attached to a three-dimensional translation stage. A

tracheotomy was performed to ensure free, natural breathing. Rectal temperatures were maintained at 38 ± 1°C with a servo-regulated heating blanket. The auditory bulla was opened and the round window membrane was exposed by using a ventral surgical approach. A glass microelectrode with a tip diameter of approximately 0.4 μm filled with 300 mM KCl was inserted into the scala media through the round window membrane and the basilar membrane. A silver/silver chloride electrode in the soft tissue of the neck served as a reference. The DC voltage between the glass electrode and the reference electrode was amplified using a BMA-200 bioamplifier (CWE, Inc., Ardmore, PA) and displayed on a digital voltmeter. The baseline level was established before the tip of the glass electrode penetrated the basilar membrane. When the tip of the microelectrode was surrounding the scala media, indicated by a sudden voltage increase, a stable DC voltage over 30 seconds was considered the EP. The recording was confirmed by demonstrating that the potential returned to approximately 0 mV when the electrode tip was retracted to the scale tympani. All data was analyzed by Student's t-test.

FUNDING

This work was supported in part by grants from the National Institutes of Health (grant numbers DC006471, DC008800, DC004554, GM60905, DK52025, 1F31DC009393, and CA21765); the Assisi Foundation of Memphis; and the American Lebanese Syrian Associated Charities of St. Jude Children's Research Hospital. J. Zuo is a recipient of The Hartwell Individual Biomedical Research Award. A. d'Azzo holds an endowed chair in Genetics from the Jewelry Charity Fund.

ACKNOWLEDGMENTS

We thank S. Bhuvanendran, S. Frase, L. Mann, and K. Murti for assistance and P. Wangemann for advice.

FIGURE LEGENDS

Fig. 1 ABR threshold elevation (dB SPL) in *Neu1*$^{-/-}$ mice at ages P21 and P60. Click ABR results were plotted in (A). *Neu1*$^{-/-}$ mice show a threshold elevation of 55 dB SPL (** P<0.001 compared to P21 *Neu1*$^{+/+}$ mice, Student's t-test) as early as P21 and 66 dB SPL at P60 (&& P<0.001 compared to P60 *Neu1*$^{+/+}$ mice, Student's t-test). No significant difference was found between P21 *Neu1*$^{+/+}$ mice and P60 *Neu1*$^{+/+}$ mice (P=0.87, Student's t-test) whereas the threshold elevation in P60 *Neu1*$^{-/-}$ mice was significantly higher than that of P21 *Neu1*$^{-/-}$ mice (# P<0.05 compared to P21 *Neu1*$^{-/-}$ mice, Student's t-test) (B) The ABR results from 8, 16, and 32 kHz tone stimuli are consistent with the click ABR results; *Neu1*$^{-/-}$ mice show a significant threshold elevation at both P21 (P<0.05, two way ANOVA) and P60 (P<0.001, two way ANOVA) compared to the control littermates. 4 *Neu1*$^{+/+}$ mice and 4 *Neu1*$^{-/-}$ mice were used at P21. 4 *Neu1*$^{+/+}$ mice and 6 *Neu1*$^{-/-}$ mice were used at P60.

Fig. 2 Hematoxylin and eosin (H&E) staining shows morphologic changes in the middle and external ear of P21 *Neu1*$^{-/-}$ mice. Arrows indicate a mild thickening of the middle ear mucosa in (C) and an infiltration of fibrocytes in the middle ear cavity (D, asterisk) in *Neu1*$^{-/-}$ mice. There was also an accumulation of cerumen occlusion in the external auditory canal (G, #) and chronic inflammatory pathologic changes in the middle ear. Scale bars: A, C, E, G: 400 μm; B, D, F, H: 150 μm.

Fig. 3 Neu1 expression pattern in the cochleae of wild-type mice. (A) Illustration of various important cell types in the cochlear scala media. Abbreviations in figure: M, marginal cell; ES,

external sulcus cell; B, Boettcher cell; OHC, outer hair cell; OP, outer pillar cell; IP, inner pillar cell; IHC, inner hair cell; IS, inner sulcus cell; ID, interdental cell; R: Reissner's Membrane. Different cell types express Neu1 in scala media (B), organ of Corti (C), and cochlear ganglion from P21 wild-type mice whereas correspondent *Neu1*$^{-/-}$ cochleae display only some background staining (D.F). Scale bar: 50 μm.

Fig. 4 Semi-thin plastic sections stained with toluidine blue show the morphologic changes in the inner ear of P21 *Neu1*$^{-/-}$ mice. Normal morphology of a P21 *Neu1*$^{+/+}$ cochlea (A). Vacuolization (arrows) is observed in many cell types, such as Reissner's membrane cells, interdental cells of spiral limbus (B), inner sulcus cell, outer hair cells, and mesothelial cells lining in the perilymphatic side of the basilar membrane (C), Boettcher cells, external sulcus cells, type-IV fibrocytes (D), and marginal cells of the stria vascularis (F). Vacuolization is most prominent in marginal cells of the stria vascularis. Vacuolization in spiral ganglia (arrowhead) and putative surrounding glial cells (asterisk) at P21 in *Neu1*$^{-/-}$ cochleae (E) is not evident. Scale bars: A: 60 μm; B, C, D, E, F: 30 μm.

Fig. 5 *Neu1*$^{-/-}$ mice show extensive vacuolization in marginal cells of the stria vascularis. (A) The darker-stained cell in the marginal cell of a P9 *Neu1*$^{+/+}$ cochlea. The flattened basal cell is at the bottom and the lighter-stain intermediate cell is located in the middle portion of the stria vascularis. (B) Vacuolization (*) in marginal cells of P9 *Neu1*$^{-/-}$ mice. (C) No vacuolization in marginal cells and basal cells in P21 *Neu1*$^{+/+}$ mice. (D) Vacuolization (*) is more extensive in marginal cells at P21 (D) than at P9 (B) in *Neu1*$^{-/-}$ mice, however vacuolization is also observed

in basal cells in P21 *Neu1*$^{-/-}$ mice (D). Abbreviations in figure: E, endolymph; M, marginal cell; I, intermediate cells; B, basal cell; C, capillary. Scale bar: 2 μm.

Fig. 6 Scanning electronic microscopy of the stria vascularis in P21 *Neu1*$^{+/+}$ (A) and *Neu1*$^{-/-}$ (B, C) mice. There are many invaginations on the surface of the stria vascularis (C, arrowheads). Scale bar: 4 μm.

Fig. 7 Changes in lysosomal membrane proteins in *Neu1*$^{-/-}$ cochleae. Left panel shows immunoblot analyses of selected lysosomal membrane and plasma membrane proteins in *Neu1*$^{-/-}$ and *Neu1*$^{+/+}$ cochleae, as indicated. GAPDH was used as a loading control. Right panel shows immunohistochemical analysis, which indicates changes in the expression of proteins in the stria vascularis in P21 *Neu1*$^{-/-}$ mice similar to those seen on the immunoblot. There is a marked increase in the expression of Lamp-1 (A, B) and Lamp-2 (C, D) mainly in the marginal cells of the stria vascularis. The dark-stained lysosomes inside the marginal cells are bubble shaped. Lamp-3 (E, F) is also present in the apical portion of marginal cells, but there is no noticeable difference in its expression in *Neu1*$^{+/+}$and *Neu1*$^{-/-}$ mice. LIMP II (G, H) is expressed in the stria vascularis and surrounding Type-I fibrocytes which is consistent with the immunoblot results. Its expression level is slightly higher in *Neu1*$^{-/-}$ mice. KCNQ1 (I, J) is expressed on the surface of the apical membrane of marginal cells. Scale bar: 40 μm.

Fig.8 Changes in the endolymphatic potential (EP) in *Neu1*$^{-/-}$ mice at ages P31–P44. The EP is 100.4 ± 11.9 mV (n = 7, mean ± SEM) in *Neu1*$^{+/+}$ mice but is 80.5± 19.1 mV (n = 6, mean ± SEM) in *Neu1*$^{-/-}$ mice ($P < 0.05$, Student's t-test).

Fig. 9 Proposed mechanisms of hearing loss in *Neu1*$^{-/-}$ mice (see Discussion for details).

References

[1] A. d'Azzo, G. Andria, P. Strisciuglio, H. Galjaard, Galactosialidosis, in: C. Scriver, A. Beaudet, W. Sly, D. Valle (Eds.), The Metabolic and Molecular Bases of Inherited Disease, vol. 3, McGraw-Hill Publishing Co., New York, 2001, pp. 3811-3826.

[2] A.C. van der Spoel, E.J. Bonten, A. d'Azzo, Processing of lysosomal β-galactosidase: the C-terminal precursor fragment is an essential domain of the mature enzyme., The Journal of biological chemistry 275 (2000) 10035-10040.

[3] G.H. Thomas, Disorders of glycoprotein degradation and structure: α-mannosidosis, β-mannosidosis, fucosidosis, and sialidosis, in: C.R. Scriver, A.L. Beaudet, W.S. Sly, D. Valle (Eds.), The Metabolic and Molecular Bases of Inherited Disease, vol. III, McGraw Hill, Inc., New York, 2001, pp. 3507-3534.

[4] E.J. Bonten, A. d'Azzo, Lysosomal neuraminidase. Catalytic activation in insect cells is controlled by the protective protein/cathepsin A, The Journal of biological chemistry 275 (2000) 37657-37663.

[5] J. Lowden, J. O'Brien, Sialidosis: A review of human neuraminidase deficiency, Am J Hum Genet 31 (1979) 1.

[6] T. Matsuo, I. Egawa, S. Okada, M. Suhtsugui, K. Yamamoto, M. Watanabe, Sialidosis type 2 in Japan. Clinical study in two siblings cases and review of literature, Journal of the neurological sciences 58 (1983) 45-55.

[7] I.D. Young, E.P. Young, J. Mossman, A.R. Fielder, J.R. Moore, Neuraminidase deficiency: Case report and review of the phenotype, Journal of medical genetics 24 (1987) 283-290.

[8] R.J. Gorlin (Ed.), Genetic hearing loss associated with endocrine and metabolic disorders, Oxford University Press, New York, 1995.

[9] J.H. Kamphoven, M.M. de Ruiter, L.P. Winkel, H.M. Van den Hout, J. Bijman, C.I. De Zeeuw, H.L. Hoeve, B.A. Van Zanten, A.T. Van der Ploeg, A.J. Reuser, Hearing loss in infantile Pompe's disease and determination of underlying pathology in the knockout mouse, Neurobiology of disease 16 (2004) 14-20.

[10] M.A. Simmons, I.A. Bruce, S. Penney, E. Wraith, M.P. Rothera, Otorhinolaryngological manifestations of the mucopolysaccharidoses, International journal of pediatric otorhinolaryngology 69 (2005) 589-595.

[11] K.K. Ohlemiller, A.K. Hennig, J.M. Lett, A.F. Heidbreder, M.S. Sands, Inner ear pathology in the mucopolysaccharidosis VII mouse, Hearing research 169 (2002) 69-84.

[12] C.L. Berry, C. Vogler, N.J. Galvin, E.H. Birkenmeier, W.S. Sly, Pathology of the ear in murine mucopolysaccharidosis type VII. Morphologic correlates of hearing loss, Laboratory investigation; a journal of technical methods and pathology 71 (1994) 438-445.

[13] P. Wangemann, Supporting sensory transduction: cochlear fluid homeostasis and the endocochlear potential, The Journal of physiology 576 (2006) 11-21.
[14] L.M. Friedman, A.A. Dror, K.B. Avraham, Mouse models to study inner ear development and hereditary hearing loss, The International journal of developmental biology 51 (2007) 609-631.
[15] B.H. Tran, Endolymphatic deafness: a particular variety of cochlear disorder, ORL; journal for oto-rhino-laryngology and its related specialties 64 (2002) 120-124.
[16] O. Sterkers, G. Saumon, P. Tran Ba Huy, E. Ferrary, C. Amiel, Electrochemical heterogeneity of the cochlear endolymph: effect of acetazolamide, The American journal of physiology 246 (1984) F47-53.
[17] K. Ikeda, J. Kusakari, T. Takasaka, Y. Saito, Early effects of acetazolamide on anionic activities of the guinea pig endolymph: evidence for active function of carbonic anhydrase in the cochlea, Hearing research 31 (1987) 211-216.
[18] N. de Geest, E. Bonten, L. Mann, J. de Sousa-Hitzler, C. Hahn, A. d'Azzo, Systemic and neurologic abnormalities distinguish the lysosomal disorders sialidosis and galactosialidosis in mice, Human molecular genetics 11 (2002) 1455-1464.
[19] G. Yogalingam, E.J. Bonten, D. van de Vlekkert, H. Hu, S. Moshiach, S.A. Connell, A. d'Azzo, Neuraminidase 1 is a negative regulator of lysosomal exocytosis, Developmental cell 15 (2008) 74-86.
[20] Y. Komura, K. Kaga, Y. Ogawa, Y. Yamaguchi, T. Tsuzuku, J.I. Suzuki, ABR and temporal bone pathology in Hurler's disease, International journal of pediatric otorhinolaryngology 43 (1998) 179-188.
[21] T. Nishi, M. Forgac, The vacuolar (H+)-ATPases--nature's most versatile proton pumps, Nature reviews 3 (2002) 94-103.
[22] M. Thorne, A.N. Salt, J.E. DeMott, M.M. Henson, O.W. Henson, Jr., S.L. Gewalt, Cochlear fluid space dimensions for six species derived from reconstructions of three-dimensional magnetic resonance images, The Laryngoscope 109 (1999) 1661-1668.
[23] R. Coenen, V. Gieselmann, R. Lullmann-Rauch, Morphological alterations in the inner ear of the arylsulfatase A-deficient mouse, Acta neuropathologica 101 (2001) 491-498.
[24] C.D. Heldermon, A.K. Hennig, K.K. Ohlemiller, J.M. Ogilvie, E.D. Herzog, A. Breidenbach, C. Vogler, D.F. Wozniak, M.S. Sands, Development of sensory, motor and behavioral deficits in the murine model of Sanfilippo syndrome type B, PloS one 2 (2007) e772.
[25] P.A. Schachern, S. Cureoglu, V. Tsuprun, M.M. Paparella, C.B. Whitley, Age-related functional and histopathological changes of the ear in the MPS I mouse, International journal of pediatric otorhinolaryngology 71 (2007) 197-203.
[26] J. Gao, S.F. Maison, X. Wu, K. Hirose, S.M. Jones, I. Bayazitov, Y. Tian, G. Mittleman, D.B. Matthews, S.S. Zakharenko, M.C. Liberman, J. Zuo, Orphan glutamate receptor delta1 subunit required for high-frequency hearing, Molecular and cellular biology 27 (2007) 4500-4512.
[27] K. Nakaya, D.G. Harbidge, P. Wangemann, B.D. Schultz, E. Green, S.M. Wall, D.C. Marcus, Lack of pendrin HCO3- transport elevates vestibular endolymphatic [Ca2+] by inhibition of acid-sensitive TRPV5 and TRPV6 channels, Am J Physiol Renal Physiol 292 (2007) F1314-1321.
[28] F.E. Karet, K.E. Finberg, R.D. Nelson, A. Nayir, H. Mocan, S.A. Sanjad, J. Rodriguez-Soriano, F. Santos, C.W. Cremers, A. Di Pietro, B.I. Hoffbrand, J. Winiarski, A.

Bakkaloglu, S. Ozen, R. Dusunsel, P. Goodyer, S.A. Hulton, D.K. Wu, A.B. Skvorak, C.C. Morton, M.J. Cunningham, V. Jha, R.P. Lifton, Mutations in the gene encoding B1 subunit of H+-ATPase cause renal tubular acidosis with sensorineural deafness, Nature genetics 21 (1999) 84-90.

[29] H. Dou, K. Finberg, E.L. Cardell, R. Lifton, D. Choo, Mice lacking the B1 subunit of H+-ATPase have normal hearing, Hearing research 180 (2003) 76-84.

[30] E.H. Stover, K.J. Borthwick, C. Bavalia, N. Eady, D.M. Fritz, N. Rungroj, A.B. Giersch, C.C. Morton, P.R. Axon, I. Akil, E.A. Al-Sabban, D.M. Baguley, S. Bianca, A. Bakkaloglu, Z. Bircan, D. Chauveau, M.J. Clermont, A. Guala, S.A. Hulton, H. Kroes, G. Li Volti, S. Mir, H. Mocan, A. Nayir, S. Ozen, J. Rodriguez Soriano, S.A. Sanjad, V. Tasic, C.M. Taylor, R. Topaloglu, A.N. Smith, F.E. Karet, Novel ATP6V1B1 and ATP6V0A4 mutations in autosomal recessive distal renal tubular acidosis with new evidence for hearing loss, Journal of medical genetics 39 (2002) 796-803.

[31] X. Wu, J. Gao, Y. Guo, J. Zuo, Hearing threshold elevation precedes hair-cell loss in prestin knockout mice, Brain research 126 (2004) 30-37.

[32] E.J. Bonten, D. Wang, J.N. Toy, L. Mann, A. Mignardot, G. Yogalingam, A. D'Azzo, Targeting macrophages with baculovirus-produced lysosomal enzymes: implications for enzyme replacement therapy of the glycoprotein storage disorder galactosialidosis, Faseb J 18 (2004) 971-973.